SUPPLEMENTARY TABLES AND FIGURES

Supplementary table 1. Overview of clinical samples and patient characteristics

Separate table in PDF

Supplementary table 2. Antibodies used for mass cytometry experiments.

Mass cytometry			
Antibodies	**Clone**	**Source**	**Identifier**
Anti-human CD45	HI30	Fluidigm	Cat# 3089003B
Anti-human CD14	Tük4	ThermoFisher Scientific	Cat# Q10064
Anti-human CD86	IT2.2	BioLegend	Cat# 305435
Anti-human CD196/CCR6	G034E3	Fluidigm	Cat# 3141003A
Anti-human CD40	5C3	Fluidigm	Cat# 3142010B
Anti-human CD278/ICOS	C398.4A	Fluidigm	Cat# 3143025B
Anti-human CD69	FN50	Fluidigm	Cat# 3144018B
Anti-human CD4	RPA-T4	Fluidigm	Cat# 3145001B
Anti-human CD8α	RPA-T8	Fluidigm	Cat# 3146001B
Anti-human CD115/CSF1R	9-4D2-1E4	Sony	Cat# 2336510
Anti-human CD16	3G8	Fluidigm	Cat# 3148004B
Anti-human CD25	2A3	Fluidigm	Cat# 3149010B
Anti-human CD54/ICAM-1	HCD54	BioLegend	Cat# 322702
Anti-human CD123/IL-3Rα	6H6	Fluidigm	Cat# 3151001B
Anti-human TCRγδ	11F2	Fluidigm	Cat# 3152008B
Anti-human CD7	CD7-6B7	Fluidigm	Cat# 3153014B
Anti-human CD95/FAS	DX2	BioLegend	Cat# 305631
Anti-human CD103	Ber-ACT8	Sony	Cat# 2351010
Anti-human CD274/PD-L1	29E.2A3	Fluidigm	Cat# 3156026B
Anti-human CD122/IL-2Rβ	TU27	BioLegend	Cat# 339015
Anti-human CD197/CCR7	G043H7	Fluidigm	Cat# 3159003A
Anti-human CD163	GHI/61	Sony	Cat# 2268010
Anti-human KLRG1	REA261	Miltenyi Biotec	Cat# 120-014-229
Anti-human CD11c	Bu15	Fluidigm	Cat# 3162005B
Anti-human CD20	2H7	BioLegend	Cat# 302343
Anti-human CD161	HP-3G10	Fluidigm	Cat# 3164009B
Anti-human CD127/IL-7Rα	AO19D5	Fluidigm	Cat# 3165008B
Anti-human CD44	BJ18	Fluidigm	Cat# 3166001B
Anti-human CD27	O323	Fluidigm	Cat# 3167002B
Anti-human CD335/NKp46	9E2	Sony	Cat# 2259510
Anti-human CD183/CXCR3	G025H7	BioLegend	Cat# 353733
Anti-human CD3	UCHT1	Fluidigm	Cat# 3170001B
Anti-human CD28	CD28.2	BioLegend	Cat# 302937
Anti-human CD38	HIT2	Fluidigm	Cat# 3172007B
Anti-human CD45RO	UCHL1	BioLegend	Cat# 304239
Anti-human HLA-DR	L243	Fluidigm	Cat# 3174001B
Anti-human CD279/PD-1	EH12.2H7	Fluidigm	Cat# 3175008B
Anti-human CD56	NCAM16.2	Fluidigm	Cat# 3176008B
Anti-human CD11b	ICRF44	Fluidigm	Cat# 3209003B

Supplementary table 3. Antibodies used for flow cytometry and cell sorting experiments.

Flow cytometry			
Antibodies	**Clone**	**Source**	**Identifier**
Anti-human CD3	SK7	BD Biosciences	Cat# 339186
Anti-human CD3	SK7	BD Biosciences	Cat# 345763
Anti-human CD4	RPA-T4	Sony	Cat# 2102660
Anti-human CD7	M-T701	BD Biosciences	Cat# 642916
Anti-human CD8α	RPA-T8	BD Biosciences	Cat# 563822
Anti-human CD14	Mφp9	BD Biosciences	Cat# 345784
Anti-human CD19	4G7	BD Biosciences	Cat# 345776
Anti-human CD25	2A3	BD Biosciences	Cat# 340907
Anti-human CD45	HI30	Life Technologies	Cat# MHCD4530
Anti-human CD45RA	HI100	Sony	Cat# 2120730
Anti-human CD45RA	L48	BD Biosciences	Cat# 335039
Anti-human CD45RO	UCHL1	Sony	Cat# 2121110
Anti-human CD56	NCAM16.2	BD Biosciences	Cat# 565139
Anti-human CD127/IL-7Rα	A019D5	Sony	Cat# 2356560
Anti-human CD127/IL-7Rα	A019D5	BioLegend	Cat# 351320
Anti-human CD103	Ber-ACT8	BD Biosciences	Cat# 550259
Anti-human KIR3DL2	#539304	R&D Systems	Cat# FAB2878P
Anti-human KIR2DL4	#181703	R&D Systems	Cat# FAB2238P
Anti-human KIR2DL1/KIR2DS1	EB6	Beckman Coulter	Cat# PN A09778
Anti-human KIR2DL3	GL183	Beckman Coulter	Cat# IM2278U
Anti-human KIR3DL1/KIR3DS1	Z27	Beckman Coulter	Cat# IM3292
Anti-human KIR2DS4	FES172	Beckman Coulter	Cat# IM3337
Anti-human NKp44	253415	R&D Systems	Cat# FAB22491P
Anti-human PD-1	MIH4	eBioscience	Cat# 12-9969-42
Anti-human PD-1	MIH4	BD Biosciences	Cat# 558694
Anti-human CD38	HIT2	eBioscience	Cat# 25-0389-42
Anti-human CD39	A1	BioLegend	Cat# 328210
Anti-human FOXP3	PCH101	eBioscience	Cat# 11-4776-71
Anti-human Perforin	δG9	BD Biosciences	Cat# 556437
Anti-human Granzyme B	GB11	eBioscience	Cat# 12-8899-41
Anti-human ICOS	C398.4A	BioLegend	Cat# 313508
Anti-human TCRγδ	11F2	BD Biosciences	Cat# 745359
Anti-human TNF-α	MAb11	eBioscience	Cat# 25-7349-82
Anti-human IFN-γ	25723.11	BD Biosciences	Cat# 341117
Anti-human IFN-γ	4S.B3	BioLegend	Cat# 502531
Live/dead	n.a.	Life Technologies	Cat# L10119

Fluorescence-activated cell sorting (FACS)			
Antibodies	**Clone**	**Source**	**Identifier**
Anti-human CD45	2D1	eBioscience	Cat# 45-9459-41
Live/dead	n.a.	Life Technologies	Cat# L10119

Supplementary table 4. Antibodies used for multispectral immunofluorescence detection.

Opal amplification			
Antibodies	**Clone**	**Source**	**Identifier**
Anti-human CD127	R34.34	Beckman Coulter	Cat# IMBULK1
Opal520	n.a.	Perkin Elmer	Cat# FP1487A

Indirect immunofluorescence detection			
Antibodies	**Clone**	**Source**	**Identifier**
Anti-human TCR V beta F1	8A3	Thermo Fisher Scientific	Cat# TCR1151
CF680 goat anti-mouse IgG1	n.a.	Biotium	Cat# 20253
Anti-human CD45RO	UCHL1	Cell Signalling Technologies	Cat# 55618
CF633 goat anti-mouse IgG2a	n.a.	VWR	Cat# 20260-1

Direct immunofluorescence detection			
Antibodies	**Clone**	**Source**	**Identifier**
Anti-human CD3*	D7A6E	Cell Signalling Technologies	Cat# 85061
Anti-human CD7	CD7-6B7	BioLegend	Cat# 343117

**CD3 was conjugated to AF594 using the Alexa Fluor 594 antibody labelling kit (Thermo Fisher Scientific).*

Supplementary table 5. Coefficient and *P*-values of immune cell correlations observed in colorectal cancer tissues (corresponding to Figure 7).

MMR-d	ILC95	ILC92	CD4memory86	CD4memory85	CD8memory96	CD8memory60	TCRγδ99	ILC97
ILC97	0.67 *(1.67E-42)*	0.65 *(1.24E-10)*	0.59 *(5.57E-07)*	0.52 *(9.77E-05)*	0.62 *(0.04)*	0.69 *(0.0002)*	0.68 *(3.78E-08)*	X
TCRγδ99	0.67 *(5.68E-11)*	0.63 *(0.001)*	0.66 *(5.96E-06)*	0.58 *(0.0029)*	0.73 *(8.98E-09)*	0.75 *(2.42E-07)*	X	
CD8memory60	0.80 *(1.43E-07)*	0.78 *(3.48E-09)*	0.89 *(3.07E-09)*	0.85 *(0.015)*	0.94 *(1.73E-08)*	X		
CD8memory96	0.72 *(0.009)*	0.72 *(0.21)*	0.85 *(0.00017)*	0.84 *(3.83E-08)*	X			
CD4memory85	0.67 *(0.0002)*	0.70 *(0.18)*	0.88 *(2.51E-08)*	X				
CD4memory86	0.73 *(2.20E-09)*	0.74 *(0.0001)*	X					
ILC92	0.82 *(6.32E-14)*	X						
ILC95	X							

MMR-p	CD4memory58	CD4memory20	Myeloid112	Myeloid88	Myeloid5	Myeloid86	Myeloid107	Myeloid1	Myeloid11	Myeloid106
Myeloid106	0.47 *(0.07)*	0.35 *(0.04)*	0.48 *(0.16)*	0.60 *(0.008)*	0.37 *(0.01)*	0.64 *(3.09E-10)*	0.50 *(0.66)*	0.55 *(0.002)*	0.68 *(1.53E-08)*	X
Myeloid11	0.30 *(0.61)*	0.22 *(0.34)*	0.38 *(0.13)*	0.43 *(0.04)*	0.28 *(0.19)*	0.52 *(0.009)*	0.35 *(0.96)*	0.37 *(0.32)*	X	
Myeloid1	0.52 *(1.37E-07)*	0.48 *(2.70E-08)*	0.43 *(0.0005)*	0.61 *(2.59E-06)*	0.52 *(7.54E-05)*	0.66 *(3.71E-07)*	0.61 *(0.38)*	X		
Myeloid107	0.67 *(0.003)*	0.57 *(0.03)*	0.59 *(0.93)*	0.60 *(0.25)*	0.55 *(0.57)*	0.67 *(0.37)*	X			
Myeloid86	0.41 *(0.004)*	0.32 *(0.0003)*	0.55 *(9.73E-05)*	0.64 *(5.62E-09)*	0.50 *(2.20E-05)*	X				
Myeloid5	0.59 *(3.53E-08)*	0.64 *(3.90E-10)*	0.62 *(0.0001)*	0.67 *(4.65E-08)*	X					
Myeloid88	0.62 *(1.23E-05)*	0.56 *(1.01E-05)*	0.64 *(3.75E-11)*	X						
Myeloid112	0.77 *(6.16E-06)*	0.65 *(1.73E-05)*	X							
CD4memory20	0.89 *(6.71E-30)*	X								
CD4memory58	X									

ILC; innate lymphoid cell, MMR-d; mismatch repair-deficient, MMR-p; mismatch repair-proficient

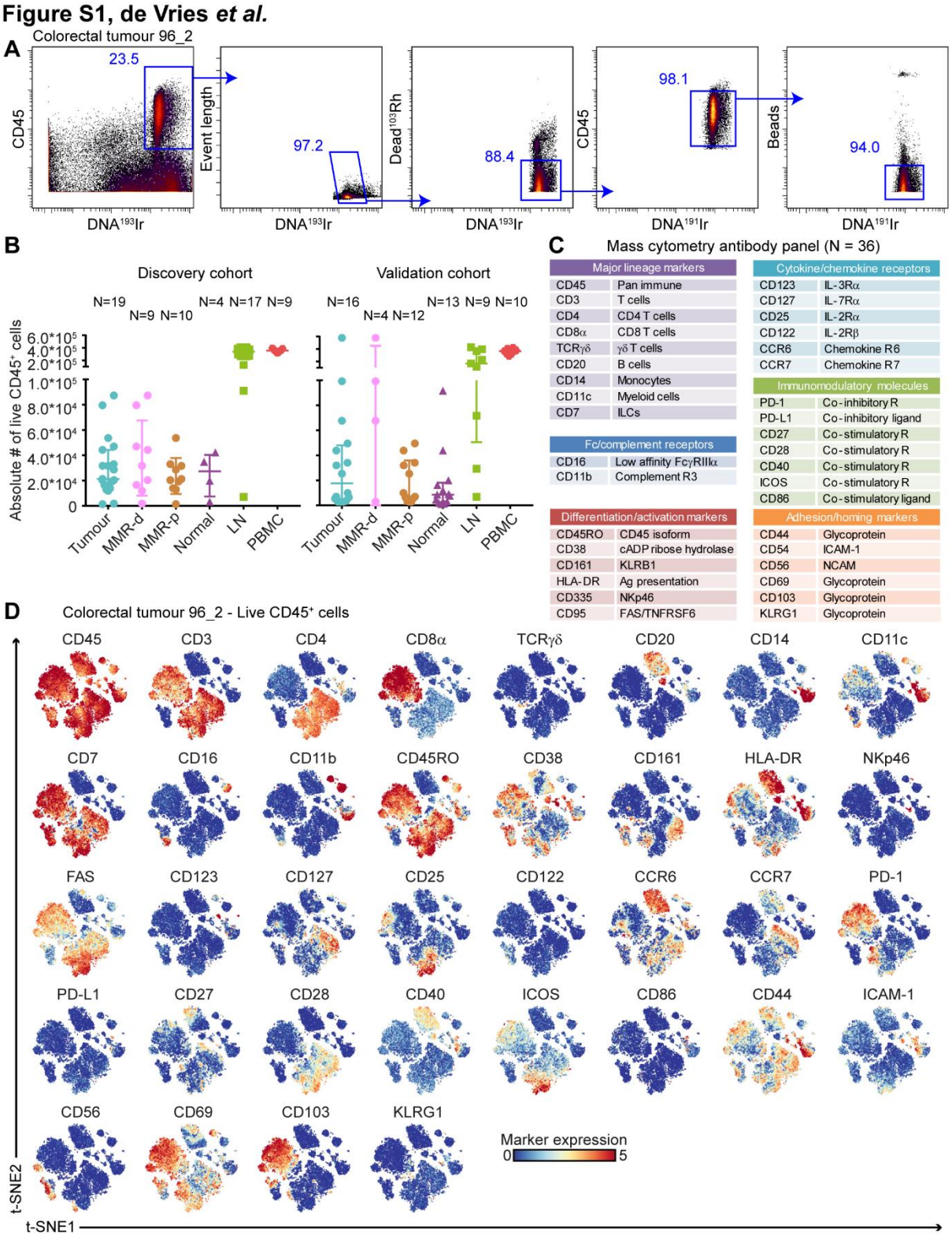

Figure S1. Mass cytometry gating strategy and antibody expression patterns.

(A) Mass cytometry gating strategy for single, live CD45^{+} cells of a representative colorectal tumour sample showing sequential gates with percentages.

(B) Absolute number of live $CD45^+$ cells of CRC tissues, colorectal healthy mucosa, tumour-associated lymph nodes, and peripheral blood samples of the discovery and validation cohort of CRC patients. Bars indicate median ± IQR. Each dot represents an individual sample. Data from 22 independent experiments with mass cytometry.

(C) Markers used to characterize immune cell phenotypes by mass cytometry.

(D) t-SNE embedding showing marker expression patterns of each antibody on single, live $CD45^+$ cells ($2.0*10^4$) from the same tumour sample as shown in (A). Each dot represents a single cell. All markers are shown with an expression range of 0-5, with the exception of CD86 (0-3) due to lower sensitivity of the metal (^{115}In).

CRC; colorectal cancer, LN; lymph node, MMR-d; mismatch repair-deficient, MMR-p; mismatch repair-proficient, PBMC; peripheral blood mononuclear cell, t-SNE; t-distributed stochastic neighbour embedding

Figure S2, de Vries *et al.*

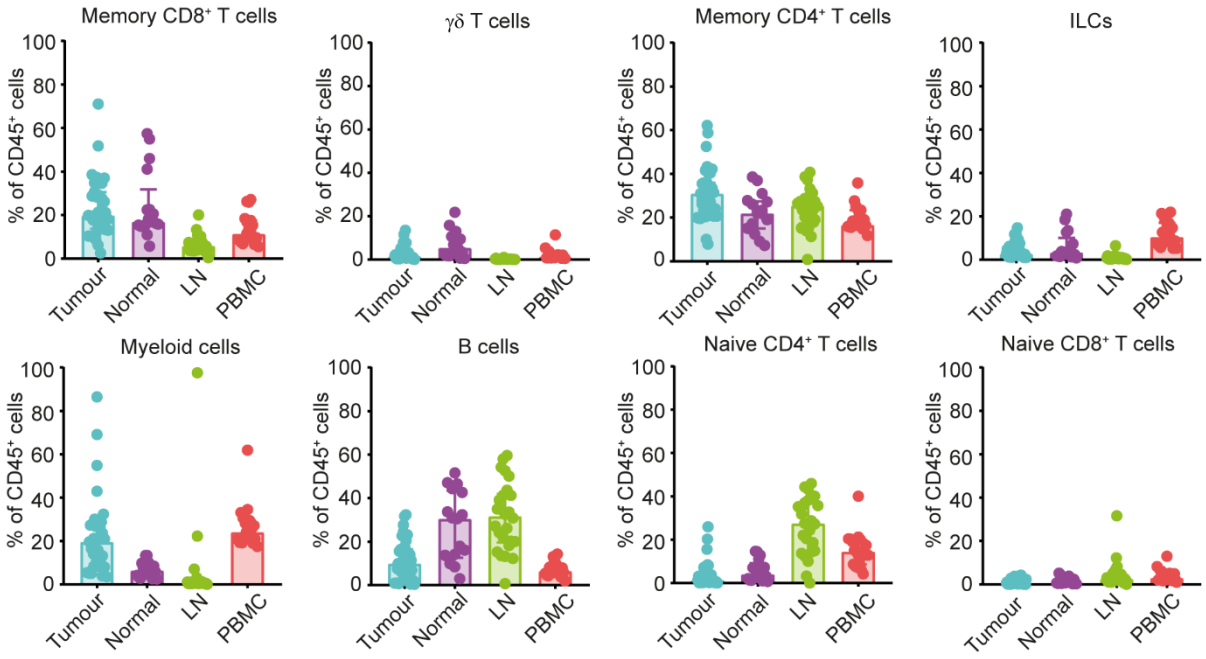

Figure S2. Major immune lineage frequencies in different tissue types of colorectal cancer patients.

Frequencies of major immune lineages across CRC tissues (N=35), colorectal healthy mucosa (N=17), tumour-associated lymph nodes (N=26), and peripheral blood (N=19) as percentage of total CD45$^+$ cells. Bars indicate median ± IQR. Each dot represents an individual sample. Data from 22 independent experiments with mass cytometry. ILC; innate lymphoid cell, LN; lymph node, PBMC; peripheral blood mononuclear cell

Figure S3, de Vries *et al.*

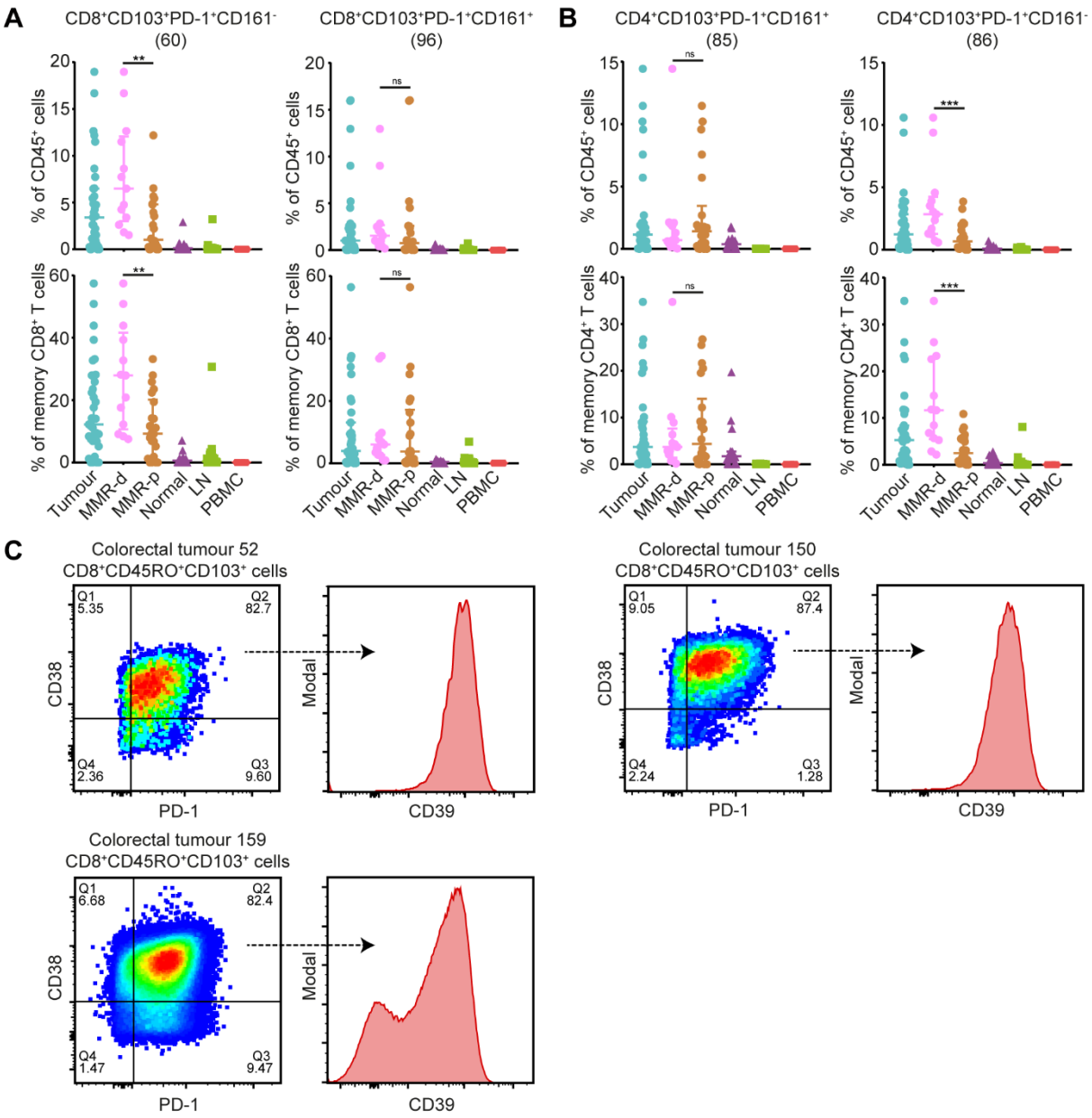

Figure S3. Characterization of tumour tissue-specific immune cell clusters corresponding to Figure 2 and 3.

(A and B) Frequencies of CD103$^+$PD-1$^+$CD161$^-$ and CD103$^+$PD-1$^+$CD161$^+$ memory CD8$^+$ T cells **(A)** and CD4$^+$ T cells **(B)** among CRC tissues (N=35, further subdivided into MMR-deficient (N=13) and MMR-proficient (N=22)), colorectal healthy mucosa (N=17), tumour-associated lymph nodes (N=26), and peripheral blood (N=19) as percentage of total CD45$^+$ cells (upper panel) and memory CD8$^+$ or CD4$^+$ T cells (lower

panel). Cluster IDs correspond to the ones in Figure 2B and 3B. Bars indicate median ± IQR. Each dot represents an individual sample. Data from 22 independent experiments with mass cytometry. NS, not significant, ***P*<0.01, ****P*<0.001 by Mann-Whitney U test.

(C) Flow cytometry plots of colorectal tumours (N=3) showing the expression of CD39 within $CD8^+CD45RO^+CD103^+PD\text{-}1^+CD38^+$ cells.

LN; lymph node, MMR-d; mismatch repair-deficient, MMR-p; mismatch repair-proficient, PBMC; peripheral blood mononuclear cell

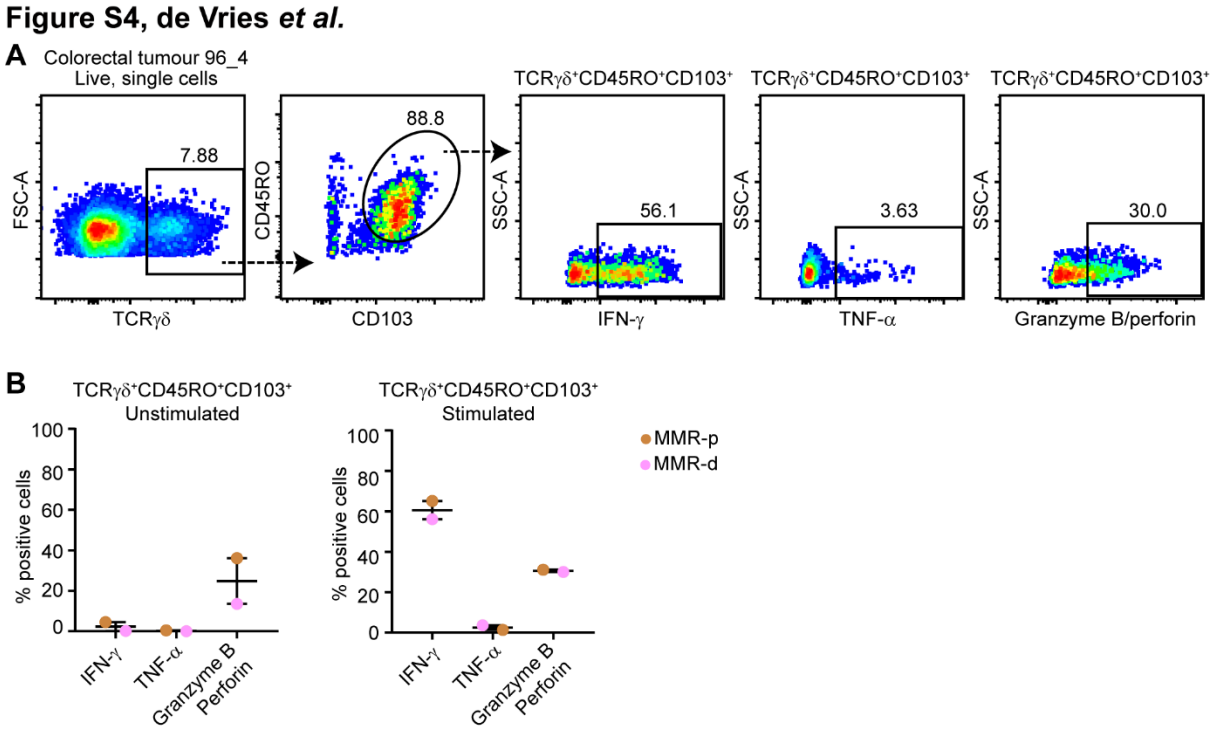

Figure S4. Tumour-resident γδ T cells are capable of producing cytokines and cytotoxic molecules upon stimulation.

(A) Flow cytometry plots of a MMR-deficient tumour sample showing the expression of cytokines and cytotoxic molecules by TCRγδ$^+$CD45RO$^+$CD103$^+$ cells upon stimulation with PMA/ionomycin.

(B) IFN-γ, TNF-α, and granzyme B/perforin expression by TCRγδ$^+$CD45RO$^+$CD103$^+$ cells from a MMR-deficient and MMR-proficient CRC with and without stimulation with PMA/ionomycin. Bars indicate median ± IQR. Each dot represents an individual sample.

MMR-d; mismatch repair-deficient, MMR-p; mismatch repair-proficient

Figure S5, de Vries *et al.*

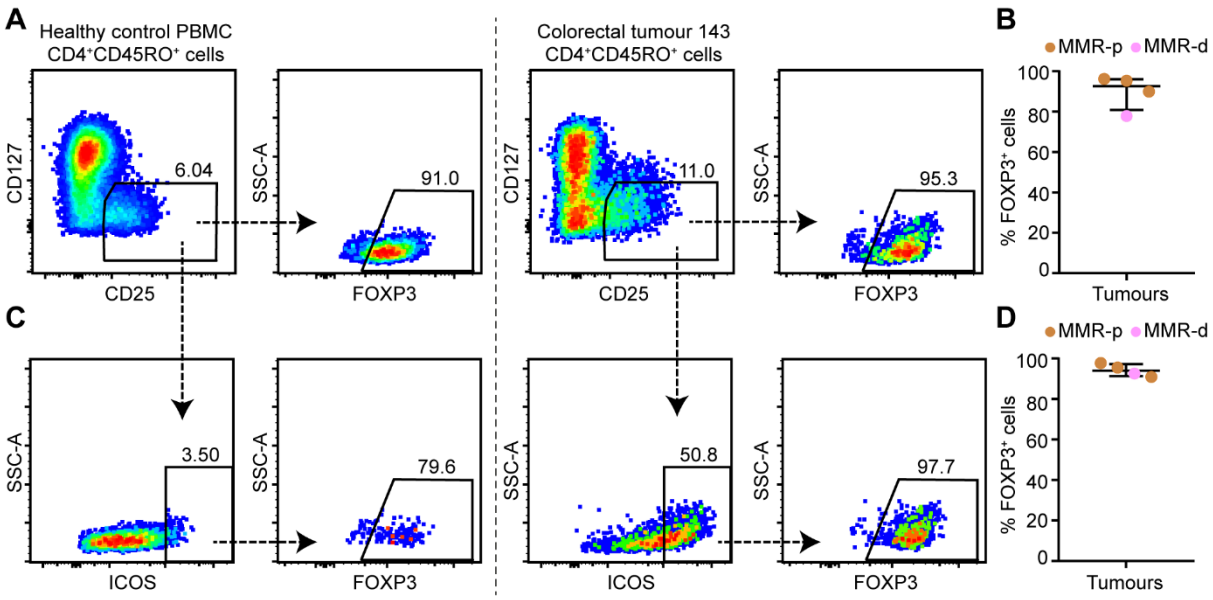

Figure S5. Expression of FOXP3 by ICOS$^+$ regulatory T cells in colorectal tumours.

(A) Representative plots of a healthy control PBMC sample and a MMR-proficient tumour sample analysed by flow cytometry showing the expression of FOXP3 by regulatory T cells (CD25$^+$CD127^{low}).

(B) FOXP3 expression in regulatory T cells (CD25$^+$CD127^{low}) from CRC tissues (N=4, of which 1 MMR-deficient and 3 MMR-proficient). Bars indicate median ± IQR. Each dot represents an individual sample. Data from two independent experiments with flow cytometry.

(C) Representative plots of a healthy control PBMC sample and a MMR-proficient tumour sample analysed by flow cytometry showing the expression of FOXP3 by ICOS$^+$ regulatory T cells (CD25$^+$CD127^{low}).

(D) FOXP3 expression in ICOS$^+$ regulatory T cells (CD25$^+$CD127^{low}) from CRC tissues (N=4, of which 1 MMR-deficient and 3 MMR-proficient). Bars indicate median ± IQR. Each dot represents an individual sample. Data from two independent experiments with flow cytometry.

MMR-d; mismatch repair-deficient, MMR-p; mismatch repair-proficient

Figure S6, de Vries *et al.*

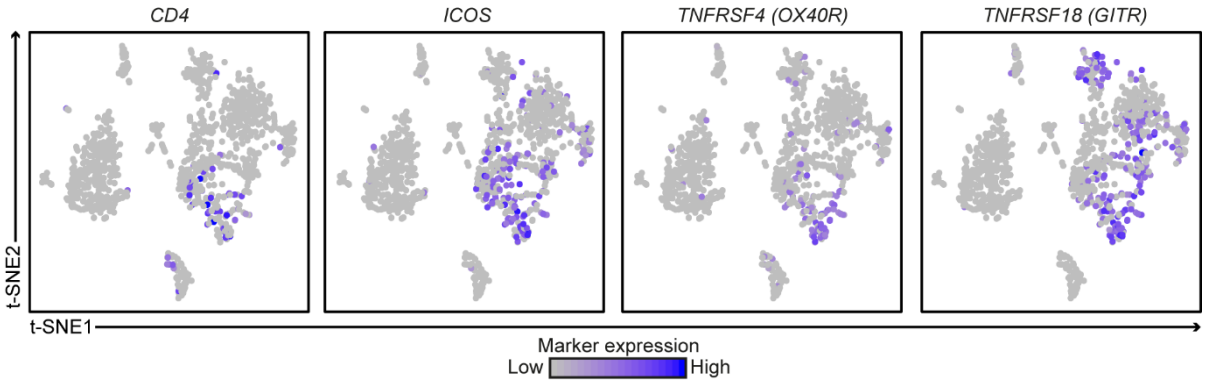

Figure S6. Co-expression of *ICOS*, *TNFRSF4 (OX40R),* and *TNFRSF18 (GITR)* on CD4^{+} T cells in colorectal cancers.

t-SNE embedding showing 1,079 cells from CRC tissues (N=7) analysed by single-cell RNA-sequencing. Colours represent the log-transformed expression levels of indicated markers. Each dot represents a single cell.

t-SNE; t-distributed stochastic neighbour embedding

Figure S7, de Vries *et al.*

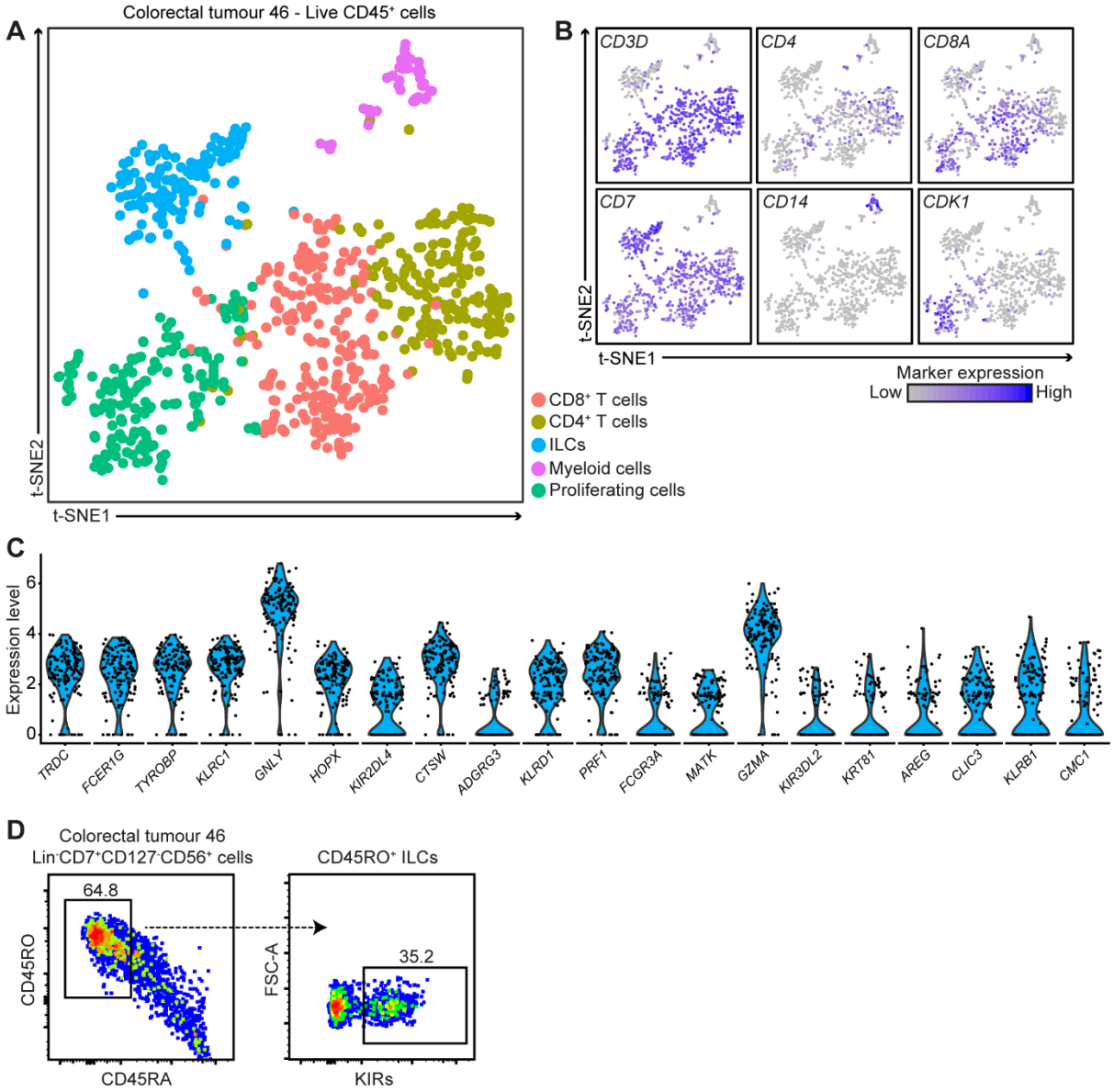

Figure S7. Expression of cytotoxic molecules and KIRs by tumour-resident ILCs.

(A and B) t-SNE embedding of single-cell RNA-sequencing data showing 795 cells from one MMR-deficient tumour that was selected for its high numbers of Lin$^-$CD7$^+$CD127$^-$CD56$^+$CD45RO$^+$ ILCs (70% of the ILC cluster) based on mass cytometry data. Colours represent the different clusters **(A)** and the log-transformed expression levels of indicated markers **(B)**. Each dot represents a single cell.

(C) Violin plot showing log-transformed expression levels of the top 20 differentially expressed genes within ILCs (N=137) as identified in (A). Each dot represents a single cell.

(D) Flow cytometry plots showing the cell surface expression of KIRs in Lin^- $CD7^+CD127^-CD56^+CD45RO^+$ ILCs from the same tumour as in (A-C).

ILC; innate lymphoid cell, KIR; killer-cell immunoglobulin-like receptor, MMR; mismatch repair, t-SNE; t-distributed stochastic neighbour embedding

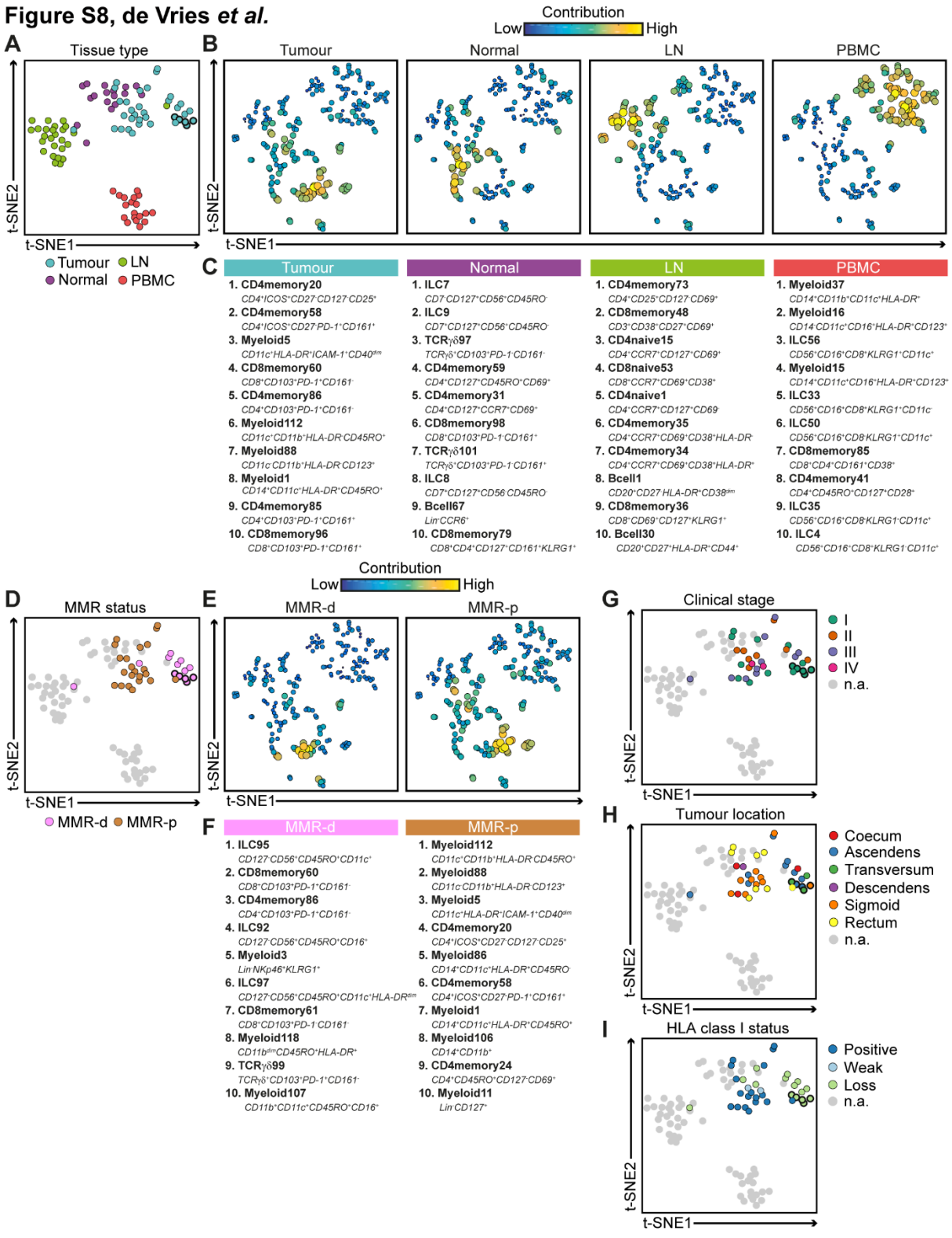

Figure S8. Integrated analysis of the immune composition in different tissue types of colorectal cancer patients.

(A) Collective t-SNE analysis showing the clustering of 97 samples based on cell percentage data (of $CD45^+$ cells) of 218 immune cell clusters. Every dot represents a sample coloured by tissue type. Five primary tumours at different locations from the same patient are highlighted. One lymph node sample clustered within the tumour samples, and was found to be infiltrated by tumour cells upon histological examination. One tumour sample clustered within the lymph node samples, and was found to contain large populations of naive $CD4^+$ T cells and B cells, which are enriched in lymph nodes. Histological examination of the tumour confirmed the presence of lymphoid aggregates with germinal centres, a Crohn-like lymphoid reaction that can be a feature of MMR-deficient tumours.[1]

(B) Collective t-SNE analysis showing the clustering of 218 immune cell clusters based on cell percentage data (of $CD45^+$ cells) of 97 samples. Every dot represents an immune cell cluster. Dot colour and size indicate the contribution of the immune cell cluster to the respective t-SNE sample signatures as shown in (A).

(C) Top ten ranked immune cell clusters contributing to the t-SNE sample signatures as shown in (A). Unique cluster IDs and a short description of their phenotype are displayed.

(D) Collective t-SNE analysis of (A) coloured by MMR status of the tumour samples.

(E) Collective t-SNE analysis of (B) showing the contribution of the immune cell clusters to the respective t-SNE sample signatures as shown in (D).

(F) Top ten ranked immune cell clusters contributing to the t-SNE sample signatures as shown in (D). Unique cluster IDs and a short description of their phenotype are displayed.

(G-I) Collective t-SNE analysis of (A) coloured by clinical stage **(G)**, tumour location **(H)**, and HLA class I status **(I)**.

HLA; human leukocyte antigen, ILC; innate lymphoid cell, LN; lymph node, MMR-d; mismatch repair-deficient, MMR-p; mismatch repair-proficient, PBMC; peripheral blood mononuclear cell, t-SNE; t-distributed stochastic neighbour embedding

Figure S9, de Vries *et al.*

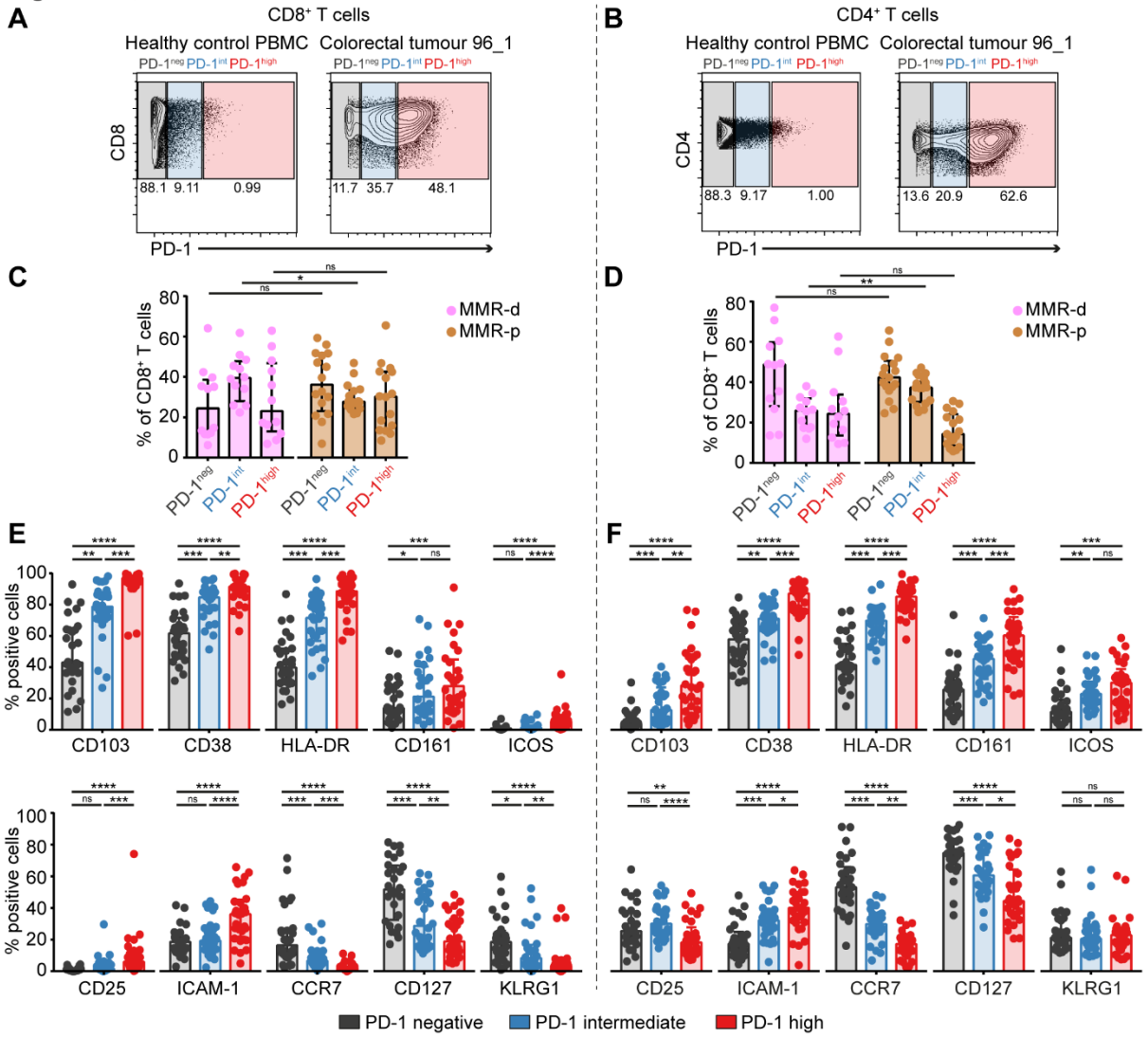

Figure S9. PD-1 expression level of CD8⁺ and CD4⁺ T cells correlates with distinct states of activation and differentiation in colorectal tumours.

(A and B) Representative plots showing the gating strategy for PD-1 negative, intermediate and high CD8⁺ T cells **(A)** and CD4⁺ T cells **(B)** in healthy control PBMC and colorectal tumour tissues (see supplementary methods).

(C) Frequencies of PD-1 negative, intermediate and high CD8⁺ T cells in MMR-deficient (N=12) and MMR-proficient (N=16) tumours.

(D) Frequencies of PD-1 negative, intermediate and high CD4⁺ T cells in MMR-deficient (N=12) and MMR-proficient (N=17) tumours.

In **C** and **D** bars indicate median ± IQR. Data from 22 independent experiments with mass cytometry. NS, not significant, *P<0.05, **P<0.01 by Mann-Whitney U-test.

(E) Frequencies of selected immune cell markers expressed by PD-1 negative, intermediate and high $CD8^+$ T cells in CRCs (N=28).

(F) Frequencies of selected immune cell markers expressed by PD-1 negative, intermediate and high $CD4^+$ T cells in CRCs (N=29).

In **E** and **F** bars indicate median ± IQR. Each dot represents an individual sample. Data from 22 independent experiments with mass cytometry. NS, not significant, *P<0.05, **P<0.01, ***P<0.001, ****P<0.0001 by Friedman test with Dunn's test for multiple comparisons.

MMR-d; mismatch repair-deficient, MMR-p; mismatch repair-proficient**,** PBMC; peripheral blood mononuclear cell

References

1. Graham DM, Appelman HD. Crohn's-like lymphoid reaction and colorectal carcinoma: a potential histologic prognosticator. Mod Pathol 1990;3:332-5.